Annu. Rev. Fluid Mech. 2005. 37:183–210
doi: 10.1146/annurev.fluid.36.050802.121940

DISSECTING INSECT FLIGHT

Z. Jane Wang
Theoretical and Applied Mechanics, Cornell University, Ithaca, New York 14853; email: z.jane.wang@cornell.edu

Key Words biofluiddynamics, unsteady aerodynamics, low Reynolds number flapping flight, forward flight, hovering, passive flight, robotic insects, computational fluid dynamics, unsteady Navier-Stokes solutions, vortex dynamics, lift, drag, efficiency

■ **Abstract** "What force does an insect wing generate?" Finding answers to this enduring question is an essential step toward our understanding of interactions of moving objects with fluids that enable most living species such as insects, birds, and fish to travel efficiently and us to follow similar suit with sails, oars, and airfoils. We give a brief history of research in insect flight and discuss recent findings in unsteady aerodynamics of flapping flight at intermediate range Reynolds numbers (10–10^4). In particular, we examine the unsteady mechanisms in uniform and accelerated motions, forward and hovering flight, as well as passive flight of free-falling objects. The results obtained by "taking the insects apart" helped us to resolve previous puzzles about the force estimates in hovering insects, to ellucidate basic mechanisms essential to flapping flight, and to gain insights about the efficieny of flight.

1. INTRODUCTION

Insects are abundant yet elusive. They are fantastic to watch but difficult to catch. From a fluid dynamics point of view, their diverse and stunning aerial acrobatics are the results of interactions between flapping wings and unsteady air flows. In the course of 350 million years, insects must have found some clever and efficient ways of interacting with fluids. Perhaps we can see the world of unsteady fluid dynamics through an insect.

Most insect wings appear as a blur. How do insects flap their wings? Equipped with newly invented slow-motion film, Marey (1868a) filmed tethered insects and also traced their wing tips using a glass hair. Although slow-motion film had a long history, it was about 90 years after Marey's study that Jensen (1956) measured the wing kinematics of tethered locust flight, which were sufficient for aerodynamic analysis. High-speed filming has evolved to digital cameras, but obtaining useful and accurate kinematics requires controlled experimental conditions, good methodology to extract relevant kinematic variables, and great deal of patience. A few complete wing kinematics (both the wing orientation and angle of attack)

have been reported for insects tethered (Jensen 1956; Nachtigall 1966, 1974) and in free flight (Fry et al. 2003).

As the wing flaps, it creates swirls of air and generates aerodynamic forces that allow insects to dart forward, to turn, and to hover. Accurately measuring the instantaneous aerodynamic forces on a live insect remains a challenge. The early measurements of averaged forces were obtained by using delicate balances (Hollick 1940, Jensen 1956, Nachtigall 1974). The time-dependent forces on a wing are trickier to measure. Previous studies used piezo-electric probe (Cloupeau et al. 1979), strain-gauge (Wilkin & Williams 1993), and the laser interference pattern (Dickinson & Götz 1996, Zanker & Götz 1990) to measure forces ranging from milligrams to grams. To deduce the force on a single wing, all four (or two) wings are presumed to behave in the same way, which is approximately true in special cases, and the wing inertia and forces on the body must be subtracted (Wilkin & Williams 1993, Cloupeau et al. 1979, Jensen 1956). These effects all contribute to the uncertainty in the measurements.

Most theoretical predictions of aerodynamic forces on an insect wing are based on the similarity and differences between an insect wing and a classical airfoil. A brief early attempt in modeling the insect wing as a rowing oar was quickly dismissed and replaced by airfoil theories (Demoll 1918, Magnan & Sainte-Lague 1933, Weis-Fogh & Jensen 1956). Choosing an airfoil rather than a rowing oar as the "zeroth-order" approximation of an insect wing has profoundly influenced the research on insect flight both in quasi-steady and unsteady regimes. It assumes that the aerodynamic lift dominates the net force and the aerodynamic drag is negligible, which needs not be the case *a priori* (Wang 2004).

In 1956, Weis-Fogh & Jensen (1956) critically reviewed experimental and theoretical work based on quasi-steady analysis (Osborne 1951, von Holst & Kuchemann 1941, Walker 1925) prior to that time. The essence of a quasi-steady analysis is the assumption that the instantaneous forces on a wing are determined by its current motion and thus do not depend on the history. For example, in the blade-element analysis, the sectional force of each blade element is determined by applying lift-drag polar to the instantaneous velocity and the angle of attack, and the net force is the sum of the sectional forces. Weis-Fogh & Jensen (1956) concluded that the often-repeated claim that "insects cannot fly according to conventional aerodynamics" (Demoll 1918, Magnan & Sainte-Lague 1933, Osborne 1951) was more likely due to incomplete data and inadequate methods rather than the failure of the quasi-steady approximations.

Although quasi-steady analysis is conceptually straightforward, verifying it in live insects is tedious. The main difficulty lies in the simultaneous and accurate measurement of the time-dependent wing kinematics, the ambient flow, the aerodynamic forces on a single wing, and appropriately measured lift-drag polar of the same wing. In a set of tour de force experiments of tethered locusts in a wind tunnel, Jensen (1956) used a high-speed single-view camera and analyzed the motion using a projection method, which gives both the velocities and the angle of attack. The wind speed is set with a feedback loop so that the tethered insects fly close

to natural flight condition. The lift- and drag-polar were measured on a dissected wing placed near the boundary layer of the wind tunnel to create a gradient flow over the wing to mimic the velocity gradient along a rotating wing. After sorting through more than 600 sets of observations and carrying out complete analysis of four sets, they concluded that the averaged force predicted by the blade-element theory is consistent with experimental measurements within the error bar. This is probably the best one can do in applying quasi-steady analysis to forward flight. In later work, Weis-Fogh (1973) further devised a quick method to analyze hovering insects and again found that averaged lift coefficients predicted by quasi-steady analysis in most hovering insects, including bumblebees, are about 1, except in dragonflies and hoverflies.

Although the quasi-steady analysis provides a simple framework for quantitative prediction of the forces in insect flight and a useful reference point with which later experimental and computational forces (Choupeau et al. 1979, Dickinson et al. 1999, Wang 2004a) can be compared, the fact that the predicted averaged lift coefficient is about 1 does not prove that insects use the steady-state principle. This view was emphasized in an extensive review of literature by Ellington (1984) and subsequent reviews (Ellington 1995, Dickinson 1996, Maxworthy 1981, Spedding 1992). There are at least four reasons to go beyond Weis-Fogh's framework. First, the experiments of Cloupeau et al. (1979) measured the unsteady forces and found that although the averaged lift in their experiments agrees with Weis-Fogh & Jensen's results, the detailed force varies from the quasi-steady prediction based on the blade-element theory. A similar discrepancy was found in a sphingid moth (Wilkin & Williams 1993). Thus, it is necessary to address the unsteady effects in order to understand the precise time course of the forces on a live insect wing. Second, other measurements of lift-drag polar of insect wings in wind tunnels (Dudley & Ellington 1990, Nachtigall 1977, Vogel 1967b) found the maximum lift coefficient less than the value reported by Jensen (1956). This discrepancy requires an explanation. Third, the anomalously high-lift coefficients (2–6) estimated for dragonflies (Ellington 1984, Norberg 1975) and hoverflies also deserves further investigation, especially considering that these insects are some of the best hoverers. Fourth, on a more general level, the insect wing motion consists of acceleration and rotation (pronation and supination), which were omitted in Weis-Fogh's quasi-steady theory. So the next natural step is to study the effects associated with these features and find out whether their effects are significant.

To probe the unsteady flows and forces on flapping wings at Reynolds number about 10^2 to 10^3, biologists developed experiments of mechanic wings dynamically scaled up from a hawkmoth (Ellington et al. 1996) and a fruit fly (Dickinson et al. 1999). In parallel, computer codes were developed to solve the Navier-Stokes equation around a moving wing. Three-dimensional (3D) general-purpose codes that have been applied to insect flight were based on the method of artificial compressibility (Liu et al. 1998, Sun & Tang 2002), the finite element method (Ramamurti & Sandberg 2002), and the immersed boundary method (Wang et al. 2003). See also articles by Mittal & Iaccarino in this volume. These methods permit prescriptions

of complex and flexible geometries. The trade-off is that they are relatively expensive and it is difficult to achieve high-order accuracy. Improvements of these methods remain to be a challenge in computational fluid dynamics. Alternatively, one can take a two-dimensional (2D) slice of the problem, which can be solved with higher-order and efficient schemes (Russell & Wang 2003, Wang 2000b), to study the basic mechanisms in flapping flight and determine whether the results compare with the experiments (Wang et al. 2004a; D. Russell & Z.J. Wang, in preparation). The development of recent tools enabled quantitative cross-comparison of flows (Wang et al. 2004a) and forces (Sun & Tang 2002, Ramamurti & Sandberg 2002, Wang et al. 2004a; D. Russell & Z. Wang, in preparation) between experiments and computations, comparison of 2D and 3D systems (Wang et al. 2004a), as well as construction of simple models of fluid forces (Minotti 2002, Pesavento & Wang 2004, Sane & Dickinson 2002). In addition, experiments inspired by flapping flight (Pesavento & Wang 2004, Vandenberghe et al. 2004; A. Andersen, U. Pesavento & Z. Wang, submitted) also offered a new perspective of the problem.

Here we review recent experimental, computational, and theoretical progress in "taking the insects apart" to scrutinize the forces and flows around a flapping wing. These new results helped us to solve some of the old puzzles, deduce intuitive pictures, and gain insights about the physical mechanisms underlying the flapping flight.

For a historical perspective of research on insect flight, see reviews by Weis-Fogh & Jensen (1956), Maxworthy (1981), Ellington (1984), Spedding (1992), and Dickinson (1996); for additional discussions of some of the literatures reviewed here, see recent reviews by Sane (2003) and Lehman (2004); for a biological perspective of insect flight, see the books by Pringle (1957), Nachtigall (1974), Brodsky (1994), Vogel (1994), and Dudley (1998); and for a more mathematical treatment of some of the classical biofluiddynamics problems, see Lighthill (1975) and Childress (1981).

2. SCALES AND THE GOVERNING EQUATIONS

The flows around birds and insects can be considered incompressible: The Mach number is typically 1/300 and the wing frequency is about 10–10^3 Hz. The governing equation is the Navier-Stokes equation subject to the no-slip boundary condition:

$$\frac{\partial \mathbf{u}}{\partial t} + (\mathbf{u} \cdot \nabla)\mathbf{u} = -\frac{\nabla p}{\rho} + \nu \nabla^2 \mathbf{u}, \tag{1}$$

$$\nabla \cdot \mathbf{u} = 0, \tag{2}$$

$$\mathbf{u}_{bd} = \mathbf{u}_s \tag{3}$$

where $\mathbf{u}(\mathbf{x}, t)$ is the flow field, p the pressure, ρ the density of the fluid, ν the kinematic viscosity, $\mathbf{u}_{bd}$ the velocity at the boundary, and u_s the velocity of the

solid. By choosing a length scale, L, and velocity scale, U, the equation can be expressed in nondimensional form containing the Reynolds number, $\mathrm{Re} = \frac{UL}{\nu}$.

There are two obvious differences between an insect wing and an airfoil: An insect wing is much smaller and it flaps. Take a dragonfly as an example. Its chord (c) is about 1cm, its wing length (l) about 4cm, and its wing frequency (f) about 40 Hz. The tip speed (u) is about 1m/s, and the corresponding Reynolds number, $\mathrm{Re} = \frac{uc}{\nu}$ about 10^3. At the smaller end, a Chalcid wasp has a wing length of about 0.5–0.7 mm and beats its wing at about 400 Hz. Its Reynolds number is about 25. The range of Reynolds number in insect flight is about 10 to 10^4, which lies in between the two limits that are convenient for theories: inviscid steady flows around an airfoil and Stokes flow experienced by a swimming bacterium. For this reason, this intermediate range is not well understood. On the other hand, it is perhaps the most ubiquitous regime among the things we see. Falling leaves and seeds, fishes, and birds all encounter unsteady flows similar to that seen around an insect.

In addition to the Reynolds number, there are at least two other relevant dimensionless parameters. A wing has three velocity scales: the flapping velocity with respect to the body (u), the forward velocity of the body (U_0), and the pitching velocity (Ωc). The ratios of them form two dimensionless variables, $\frac{U_0}{u}$ and $\frac{\Omega c}{u}$, the former is often referred to as the advance ratio, and it is also related to the reduced frequency, fc/U_0.

3. WING MOTION

3.1. Observations

If an insect wing is rigid, for example, a *Drosophila* wing is approximately so (Vogel 1967a), its motion relative to a fixed body can be described by three variables: the position of the tip in spherical coordinates, ($\Theta(t)$, $\Phi(t)$), and the pitching angle $\Psi(t)$, about the axis connecting the root and the tip. This representation is used by Wang et al. (2003), Wakeling & Ellington (1997), and Zanack (1972) in their experimental measurements. To estimate the aerodynamic forces based on blade-element analysis, it is also necessary to determine the angle of attack (α). The typical angle of attack at 70% wingspan ranges from 25° to 45° in hovering insects (Ellington 1984), and about 15° in hummingbirds (Jensen 1956). Despite the wealth of data available for many insects, relatively few experiments report the time variation of α during a stroke. They include wind tunnel experiments of a tethered locust (figure III. 8 in Jensen 1956) and a tethered fly (figure 26 in Nachtigall 1966), and free hovering flight of a fruit fly (figure 2 in Fry et al. 2003). The stroke angle is described well by a sinusoidal motion or the first few Fourier modes (Fry et al. 2003, Wakeling & Ellington 1997; D. Russell & Z. Wang, in preparation), but the angle of attack is relatively constant after pronation and supination. Figure 1 shows the wing motions of a tethered dragonfly recently taken in our lab (D. Russell & Z. Wang, in preparation).

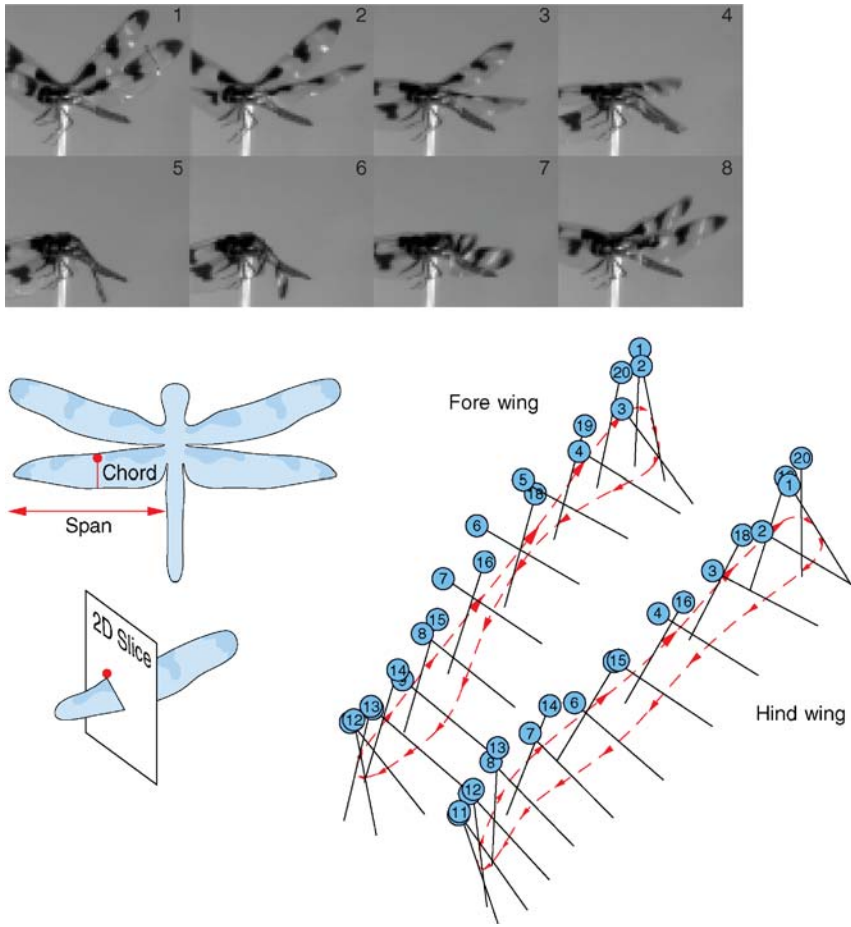

Figure 1 Top: tethered dragonfly during one wing beat, filmed at 1600 frames per second. The three-dimensional wing kinematics is extracted from two simultaneous views using a mirror. Lower right: the chord positions of fore and hind wing projected onto a two-dimensional slice (*lower left*) (D. Russell & Z. Wang, in preparation).

Because they are relatively easy to measure, the wing-tip trajectories have been reported more frequently. Marey (1868a) saw a figure eight, which was later argued to be an artifact of tethered flight. For example, Hollick (1940) selected only flight sequences that produced enough lift to support a weight, and found the wing tip followed an elliptical shape. Noncrossing shapes were also reported for other insects (Ellington 1984; Fry et al. 2003; Jensen 1956; Nachtigall 1966, 1974; Willmott & Ellington 1997a). Regardless of their exact shapes, the plugging-down motion indicates that insects may use aerodynamic drag in addition to lift to support its weight (Wang 2004). This role of lift and drag will be discussed in sections 8.3 and 9.

An insect wing is not entirely rigid, as evident in the still images of insects in natural flight (Dalton 1975). Some wings twist along the span similar to a helicopter blade; the angle of attack is the greatest at the wing base and decrease toward the tip (see review by Ellington 1984). For a helicopter wing, such a design ensures that the effective angle of attack is the same along the wingspan. In a few insects, hoverflies, flies, and butterflies, a torsional wave, where the wave progresses toward the wing base, was reported.

Wing interactions are most evident during clap-and-fling of a small wasp *Encarsia Formosa* discovered by Weis-Fogh (1973). A high Reynolds number version of this interaction was investigated by Lighthill (1973) and Maxworthy (1979). The readers are refered to the previous annual review by Maxworthy (1981) for details. The clap-and-fling is also often seen in butterflies. Another kind of interaction is the fore- and hind-wing interaction seen in dragonfly flight, indicated by the variations of the phase-relation between them during different maneuvers (Alexander 1984, Ruppell 1989). Computations of Sun & Lan (2004) showed that the fore-hind wing interaction is weak and can even be detrimental to the net vertical force generation. Russell & Wang (in preparation) noted similarly weak dependence in term of the force; however, they found that the hovering efficiency can be improved by modulating the phase relation between the fore and the hind wing.

3.2. Prescribed Motions

Many recent studies focused on prescribed motions that are designed to capture the main features of the flapping motions seen in insects. They include back and forth strokes along a horizontal (section 8.2) or an inclined (section 8.3) stroke plane, as well as up and down strokes against wind (section 7).

3.3. Free Motions

A different approach to flapping flight is to set the wing free and let it flap or fly in response to its interaction with the fluids. Partially free flapping motions have been studied in the context of a silk thread suspended in soap film (Zhang et al. 2000), symmetry breaking in a vertically oscillating wing (Vendenberghe et al. 2004), fish motion behind a cylinder (Liao et al. 2003), and a pair of wings driven by periodic forces applied to the roots (Wang et al. 2003). A fully passive flight was studied in free-falling paper and plates (Pesavento & Wang 2004; A. Andersen, U. Pesavento & Z. Wang, submitted).

4. CLASSICAL THEORY OF AERODYNAMIC FORCES

A wing moving in fluids experiences a fluid force. Following the convention in aerodynamics, the force component normal to the direction of the far field flow relative to the wing is referred to as lift (L), and the force component in the opposite

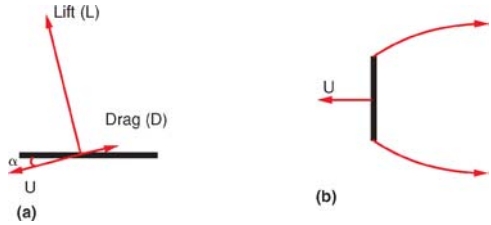

Figure 2 (*a*) Definition of aerodynamic lift and drag, (*b*) a stalled plate with velocity discontinuity springing from both edges of the plate as in the theory of Kirchhoff, Helmholtz, and Rayleigh.

direction of the flow is drag (D) (Figure 2*a*). At the Reynolds numbers considered here, an appropriate force unit is $\frac{1}{2}\rho U^2 S$, where ρ is the density of the fluid, S the wing area, and U the wing speed. The dimensionless forces are called lift (C_L) and drag (C_D) coefficients,

$$C_L(\alpha) = \frac{L}{\frac{1}{2}\rho U^2 S}, \qquad C_D(\alpha) = \frac{D}{\frac{1}{2}\rho U^2 S}. \tag{4}$$

C_L and C_D are constants only if the flow is steady.

A special class of objects such as airfoils may reach a steady state when it slices through the fluid at a small angle of attack. In this case, the inviscid flow around an airfoil can be approximated by a potential flow satisfying the no-penetration boundary condition. The Kutta-Joukowski theory of a 2D airfoil further assumes that the flow leaves the sharp trailing edge smoothly, and this determines the total circulation around an airfoil. The corresponding lift is given by Bernoulli's law (Blasius theorem):

$$C_L = 2\pi \sin\alpha, \qquad C_D = 0. \tag{5}$$

Detailed calculations can be found in most fluid dynamics textbooks (see, for example, Glauert 1947, Prandtl & Tietjens 1957, von Karman & Burgers 1963). Back-of-envelope calculations based on particles bouncing off the plate, as was used by Newton, would predict a $\sin^2\alpha$ dependence, much smaller than the actual lift at small α. This would eliminate planes and birds as flying machines. What was not captured in Newton's theory is the singular change of the flow near the edges of the plate when the wing tilts up just slightly against the flow. This singular change was modeled mathematically by the Kutta condition in the Kutta-Joukowski theory.

The steady state typically exists up to an angle of about 15°, above which the flow separates, the lift drops, the drag increases, the airplane stalls, and the theory fails. To know when stall happens, wind-tunnel experiments are carried out to measure the lift-drag characteristics. For each airfoil, a lift-drag polar (lift plotted against drag with α marked on the curve) is pretty much all there is to know about

its performance. For example, one can read off the gliding angle or its efficiency in forward flight, both of which are related to the lift-to-drag ratio at a fixed angle.

The second special case is a plate moving in the direction almost normal to itself (Figure 2*b*). The theory of Kirchhoff, Helmholtz, and Rayleigh assumes that the velocity discontinuity springs from both edges of the plate. Behind the plate is a region of dead water. This predicts a force normal to the plate (von Karman & Burgers 1963),

$$C_L = \pi \sin 2\alpha/(4 + \pi \sin \alpha) \quad (6)$$

$$C_D = \pi \sin^2 \alpha/(4 + \pi \sin \alpha). \quad (7)$$

Because it assumes the pressure behind the plate to be the same as that at infinity, which is an overestimate, it under-predicts the drag.

Many classical unsteady airfoil theories are further developments of the Kutta-Joukowski theory. For example, Wagner (1925) and von Karman & Sears (1938) developed theories for nonuniform motion. For a review of modeling of aquatic and animal locomotion employing classical theories, see Lighthill (1973) and Wu (2001).

5. AERODYNAMIC FORCE DETERMINED FROM A VORTEX WAKE

The force on a wing can, in theory, be determined by tracking the flow momentum in the wake. This view of momentum balance was useful in studies of helicopters and is also adopted theoretically (Ellington 1984; Rayner 1979a, 1979b) and experimentally (Freymuth et al. 1991, Spedding et al. 2003) to calculate the force in flapping flight. General formulas relating aerodynamic forces and moments to rates of change of vorticity moments in the fluid were derived in Wu (1981). The appeal of this approach is that one does not have to follow the details of the wing motion and wing shape. The vortex wake is a "footprint" of a traveling insect and gives an intuitive picture of the net force, as is seen in Figures 4 and 6. On the other hand, it is quite a task to track all the splashes in a fluid and thus difficult to obtain accurate quantitative measurements. The forces reported in the following sections are direct measurements on a wing or computed by integrating the stress tensor along the wing surface.

6. QUANTIFYING UNSTEADY AERODYNAMIC FORCES

A wing moving in an arbitrary manner inevitably falls outside the conditions required by classical theories. For example, an insect wing motion differs from a translating or rotating classical airfoil in at least three respects: (*a*) the mean angle of attack during each half stroke is higher than the stalled angle, (*b*) the

wing reverses its course and pitches periodically, and (*c*) the wing accelerates and decelerates near wing reversal. The following sections describe recent experimental and computational work in understanding the consequences of these differences.

6.1. Unsteady Force on a Steady Translating Wing

In general, the force on a steady translating wing is unsteady at sufficiently high Reynolds numbers. A familiar example is flow past a cylinder or an inclined plate, where the wake consists of a train of von Karman vortices. Thus C_L and C_D are no longer constants, but functions of time. The steady-state C_L and C_D measured wind-tunnel experiments are the averaged values in the von Karman shedding state. To follow the time history of force for a plate starting from rest, either a towing tank or direct numerical simulations is needed.

Francis & Cohen (1933) measured the transient lift on a stalled airfoil in a towing tank and found that its peak value was about 50% higher than the maximum steady-state value obtained in a wind tunnel. This brief lift enhancement is associated with the formation of the leading-edge vortex on the upper surface of the wing before it rolls off, a phenomenon known as the dynamic stall.

The Reynolds number in the experiment of Francis & Cohen (1933) was about 10^5. To investigate dynamic stall at low Reynolds number (about 200), typical of a fruit fly, Dickinson & Götz (1993) measured the transient forces on an impulsively started plate and compared the instantaneous force coefficients after 2 and 7 chords of travel. The difference between the two is small below the angle of attack 13.5°, above which the force measured at 2 chords is higher. At the maximum lift, the difference is about 50%.

One can also run a similar towing experiment on a computer sufficiently long to reach the shedding state so that the transient value can be compared with the averaged values in the shedding state. Figure 3 shows computed flow and forces around an impulsively started ellipse at angle of attack $\alpha = 40^\circ$ and at $\mathrm{Re} = 1000$ moving over 20 chords (Wang 2000b). The sharp gradient in region A is due to the impulsive start. Region B corresponds to the rollup of the vortex sheet near the tips of the ellipse. Region C shows a temporary plateau in the force before the leading-edge vortex is shed, and region D shows the periodic force associated with the von Karman wake. The onset of the shedding in this case occurs in about 4 chords of travel, which is consistent with that found by Dickinson & Götz (1993). The difference between the force in the plateau and the averaged value in the shedding state is again about 50%.

Early measurements on insect wings were typically obtained in wind-tunnel experiments and thus are averaged values in the shedding state. An insect wing reverses periodically and, thus, may not experience the steady-state value. We come back to the timescale for the onset of vortex shedding in the discussions of the stability of the leading-edge vortex in section 6.2 and variations of flapping frequency with wing size in Section 7.

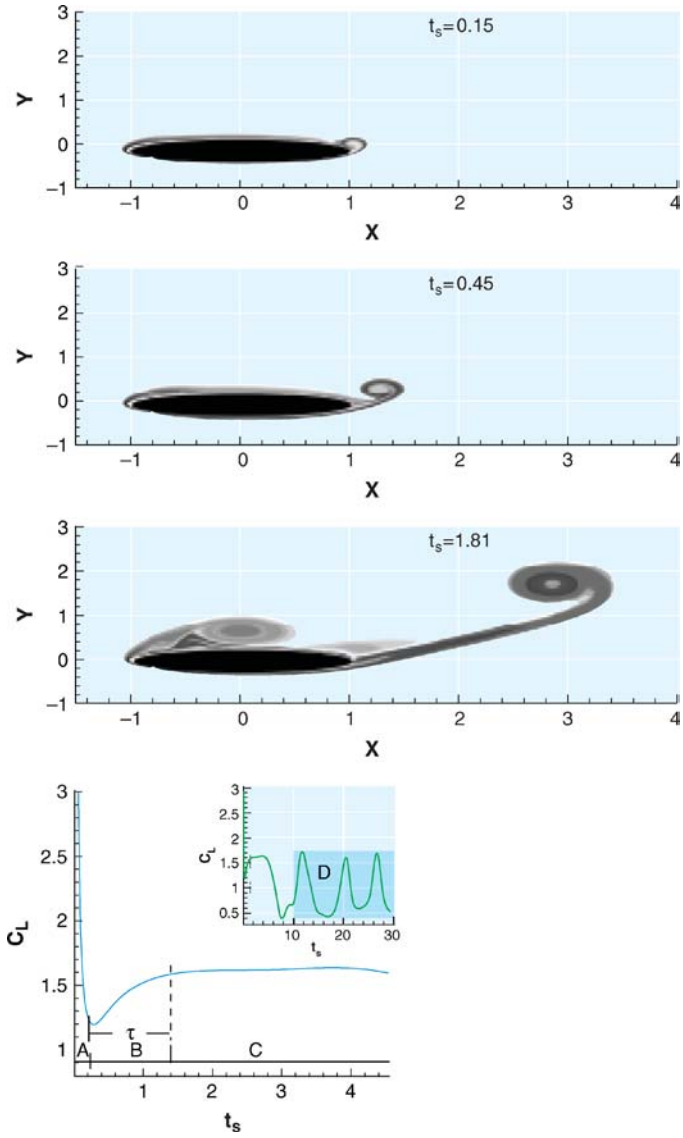

Figure 3 An impulsively started ellipse of aspect ratio $^1/_8$ with an angle of attack 40° and Re = 1000. Top: Vorticity contour plot. Bottom: Lift coefficient in the dynamic stall regime. Inset: Lift coefficient over a longer time period, up to the von Karman shedding state (Wang 2000b).

6.2. Two-Dimensional Translating Wing versus Three-Dimensional Flapping Wing About its Root

An insect wing flaps about its root while translating forward. Thus, unlike a linearly translating wing, it has a velocity gradient along the wingspan. This difference between a flapping and a translating wing has been under much discussion recently after Ellington and coworkers (Ellington et al. 1996, Willmott & Ellington 1997a) observed a conical leading-edge vortex with a strong spanwise flow on a dynamically scaled-up mechanic hawkmoth wing at Re $\sim$ 5000. Many discussions in the recent literature refer to this spanwise flow as the 3D effect of a flapping wing, which is different from the 3D end effects often discussed in a translating airfoil. In the flapper experiment, the leading-edge vortex remains stable until just after the mid-stroke, and then it breaks down at 60% to 70% span. The tip region separates from the wing during the latter half of the down stroke (Ellington et al. 1996). The conical-shape vortex was previously seen in Maxworthy's (1979) experimental study of clap-and-fling mechanism using two delta wings. Birch & Dickinson (2001) observed a much smaller spanwise flow, about 2% to 5% of the tip velocity over a dynamically scaled mechanic fruit fly wing at Re $\sim$ 150. In their case, the leading-edge vortex is robust; inserting fences to partition the leading edge resulted in no significant alteration of the forces. The difference between these two experiments may be due to the difference in the Reynolds number.

Another notable difference between a revolving wing and a translating wing is the absence of von Karman vortex shedding in the case of a revolving wing even after a full rotation (Dickinson et al. 1999, Usherwood & Ellington 2002a). Two hypotheses have been given. Ellington et al. (1996) suggested that the spanwise flow convects the vorticity out to the wing tip and prevents the leading-edge vortex from accumulating into a large vortex that would be unstable in two dimensions. This effect of spanwise flow was also discussed in the stall characteristics of a rotor blade under somewhat different conditions (Harris 1996, Schlichting 1979), where the data was taken for angle of attack typically less than 20°. Observing relatively small spanwise flow in their experiment, Birch & Dickinson (2001) suggested that the downwash would reduce the effective angle of attack and thus enhance the leading-edge stability. Here we suggest that the absence of the von Karman wake may also be a consequence of the fact that the velocity at the root is zero in these experiments. The vortex line is pinned to the root and cannot shed. If the revolving wing is translating at U_0, as with forward flight, one expects that the timescale associated with shedding is inversely proportional to U_0 and that the conical shape becomes more cylindrical. This might explain the cylindrical leading edge seen on a forward-flying butterfly wing (Srygley & Thomas 2002).

Although a continuously revolving wing is of interest in its own right, it is different from a flapping wing fixed at the root. In the latter case, the wing reverses periodically and a new leading-edge vortex is generated in each half stroke. Whether an insect wing can take advantage of the dynamic stall depends on the relative values of the flapping period and the transient timescale associated with

dynamic stall, or equivalently, of the distances traveled in these two timescales. Hovering flight compiled by Weis-Fogh (1973) (in his table 4) shows that the ratios of stroke-arc to wing-chord of different species, including bats, birds, butterflies and moths, wasp and bees, and flies, have values less than 4. Beetles have values between 5 and 6. These are comparable with the transient scale seen in a 2D translational wing, shown in Figure 3, and also, curiously, with the timescale seen in the vortex ring generation (Mohensi & Gharib 1998). One then expects that these insects can take advantage of dynamic stall even in 2D without the absolute stability of the leading-edge vortex (Wang et al. 2004a).

Computed forces on a 2D and 3D flapping wing show relatively small differences, despite the differences in the leading-edge vortex structures. For example, Sun & Lan (2004) found that the force on a 3D dragonfly wing matches those forces obtained in 2D computations (Wang 2000a). The averaged vertical force coefficient in 3D is about 20% less than in 2D. The smaller value in 3D is consistent with the classical picture of lift reduction due to the tip vortex. In addition, Wang et al. (2004a) found good agreement between forces and flow (Figure 4) in experiments and 2D computations in a family of normal hovering.

6.3. Lift-Drag Polar at Full Range of Angle of Attack

Given that lift and drag are functions of time, the classical lift-drag polar cannot do full justice to the complexity of force and flow. Nonetheless, it is instructive to see the difference in the values obtained under different conditions for different wings, as compiled in figure 9 of Sane (2003). Overall, 2D steady-state averaged force is smaller than 2D max transient force by about 50%, as explained in section 6.1, 2D transient forces are roughly the same as 3D transient forces up to an angle of attack about 72°, and 3D transient forces are roughly the same as 3D steady-state forces. Three-dimensional steady force is slightly lower than 2D transient force, likely because of downwash due to tip vortices. An empirical fit of a semi-elliptical lift-drag polar in the full range of angle of attack can be described by (Wang et al. 2004a)

$$C_L = A \sin 2\alpha, \tag{8}$$

$$C_D = B - C \cos 2\alpha, \tag{9}$$

where A, B, and C are constants that depend on the Reynolds number, the wing shape, etc. At small α, $\sin 2\alpha \sim 2 \sin \alpha$ and the 2α dependence is consistent with the symmetry of a plate and with the theoretical prediction of lift and drag of a stalled wing.

The maximum lift coefficient on an insect wing obtained in most wind-tunnel measurements was less than 1 (Dudley & Ellington 1990, Nachtigall 1977, Vogel 1967b) except for Jensen's (1956) results. The key difference between Jensen's and other wind-tunnel experiments is that he placed the wing near the boundary layer to simulate the gradient of velocity on a rotating wing. Usherwood & Ellington

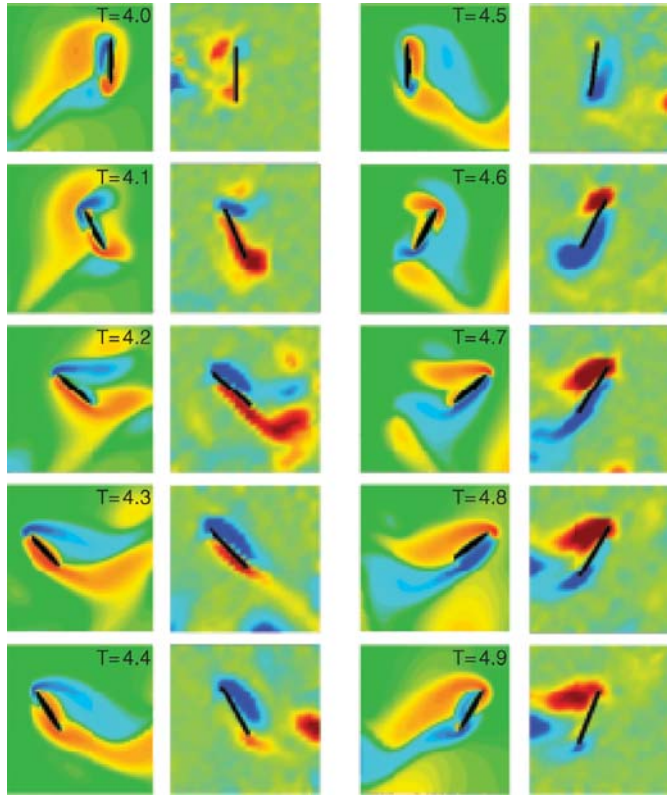

Figure 4 Comparison of computed vorticity in a normal hovering against robotic wing experiments. Re = 150. The end-to-end amplitude to chord ratio is 4.8. Ten frames are shown in the fourth stroke. Red corresponds to counter-clockwise rotating vortices and blue clockwise rotating vortices. The wing is in black. The first and third columns are computed vorticity, and the second and fourth columns are digital particle image velocimetry data in a two-dimensional slice at 65% span of a robotic wing. The time sequence is indicated by the numbers on each plate (Wang et al. 2004a).

(2002b) suggested that Jensen was effectively measuring the steady-state drag polar of a revolving wing, which has a value closer to the transient force.

6.4. An Acceleration Wing

In a reciprocal motion, a wing must decelerate and accelerate. For power-law impulsively accelerated flow, it is possible to obtain some analytical approximations. The force on a linearly accelerating airfoil was first analyzed by Wagner (1925) using a conformal mapping method. For an impulsively started wing, it predicts

a delay in acquiring the final steady-state circulation and lift, which were verified experimentally (Walker 1931). For a linearly accelerating wing, it predicts an initial force that is the sum of the half of the quasi-steady-state lift plus an added mass, which compares well with the direct numerical simulations (Pullin & Wang 2004).

Wagner's theory was meant to be applied to small angle of attack. To treat the full range of angle of attack, both the leading- and trailing-edge vortex sheets must be included. Jones (2003) formulated the separated flow around a moving plate using a regularized boundary-integral representation and obtained numerical solutions at angles of attack close to 90°. Pullin & Wang (2004) were able to obtain an analytic approximation of the forces at all angles of attack by modeling the leading- and trailing-edge vortices with self-similar spiral vortex sheets (Pullin 1978). Their theory provides a good prediction of the force (both lift and drag) at large angle of attack, and it also predicts a singular time dependence of the force coefficients at $t = 0$, which may be related to parts of force peaks seen near the wing reversal in hovering motions (section 8.2).

7. FORWARD-FLAPPING FLIGHT

An up-down symmetrically flapping wing can fly into a head wind, and this provides a basis for forward flight at high Reynolds numbers. This nonintuitive result can be explained by the fact that the aerodynamic force is roughly normal to the relative flow when the Reynolds number is sufficiently high. The aerodynamic lift has a forward component in both the up and down strokes (Figure 5). Alternatively, the signature of thrust can be seen in the wake of a flapping wing, which consists of a reversed von Karman wake (Figure 5) that carries the fluid momentum away from the wing, thus propelling the wing forward (von Karman & Burgers 1963). Classical analysis for forward flight can be found in Glauert (1929). Below we focus on two lessons drawn from the studies of the simplest form of forward flight related to the understanding of insect flight.

7.1. Transitional Reynolds Number and Symmetry Breaking

In Stokesian regime ($\mathrm{Re} = 0$), the up-down symmetric flapping discussed above generates a drag instead. How large does the Reynolds number have to be so that the same motion generates a thrust? Or roughly how big does an organism have to be so that it can fly forward by flapping up and down? To investigate the critical Reynolds number for the onset of the thrust, Childress & Dudley (2004) examined the swimming speed of swimming mollusc which use both ciliated surfaces and a pair of flapping wings. They found that the flapping dominates the locomotion above Reynolds number in the range of 5–15. Their analysis of the theoretical model based on the Oseen equation further suggested that the transition from Stokesian realm to forward flight should be regarded as bifurcation from rest with

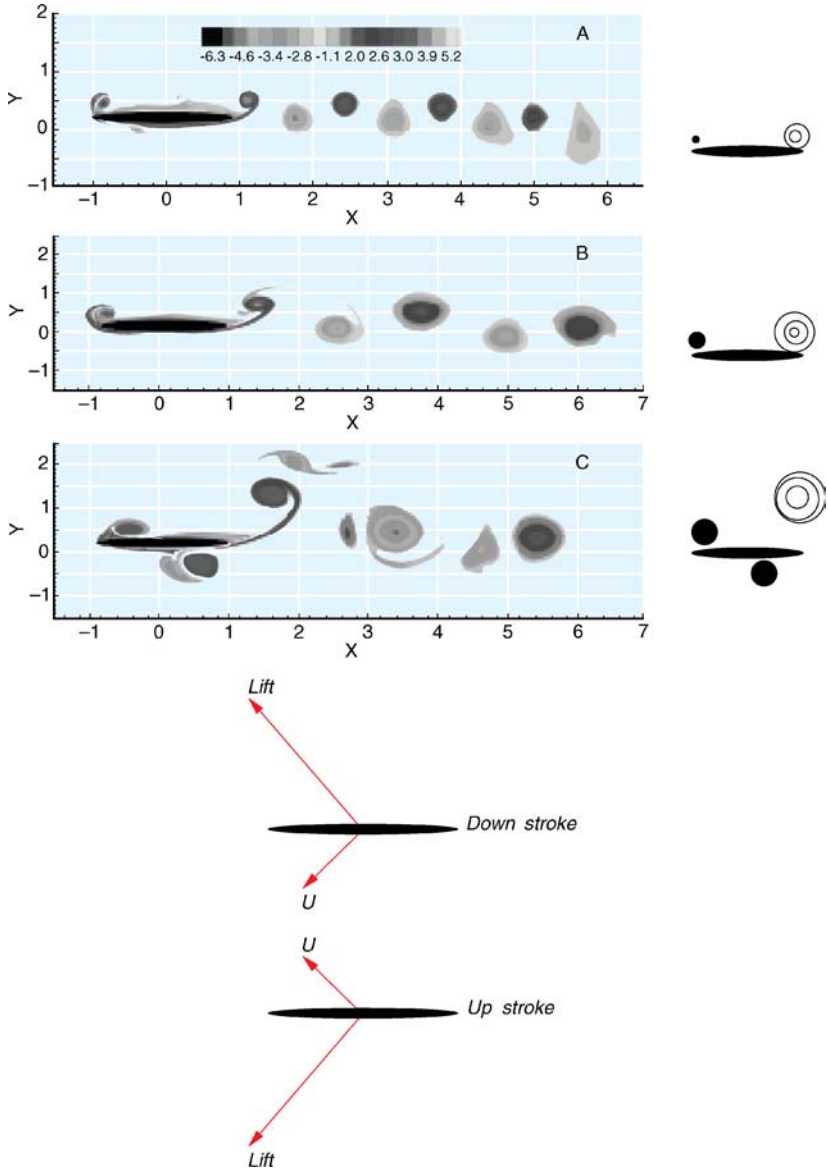

Figure 5 Forward flight. Top: Vorticity field (reversed von Karman wake) shed by a symmetric flapping wing in forward flight at three frequencies (Wang 2000b). Bottom: The schematic of the thrust generation, which is the forward component of aerodynamic lift.

respect to $\mathrm{Re}_\omega = \frac{\omega c^2}{\nu}$. The experiments of a symmetric oscillating plate show the transitional value to be about 20–55 (Vandenberghe et al. 2004). In the experiment, the wing finds its own equilibrium forward flight speed above the critical Re_ω. The effect of Reynolds number (Re) on the thrust was also studied in (Wang 2000a and Miller & Peskin 2004).

A related symmetry breaking is studied in a butterfly model (Iima & Yanagita 2001).

7.2. Flapping Frequency and Timescale for Vortex Shedding

Birds and fish flap more slowly than insects, which are smaller. The same inverse relation occurs in insects. The data compiled by Greenewalt (1962) show such an inverse scaling with the exponent about 1 over a size range of 3 decades. The flapping frequency no doubt is dictated by muscle frequency, but because the wing is also coupled to the fluid, it is worth asking whether there is an aerodynamic basis for such a scaling. To investigate this, Wang (2000b) studied the force generation in a family of symmetric flapping motion and found that the averaged thrust is maximal at a fixed reduced frequency $St_c = \frac{fc}{U_0}$. Because U_0 was kept constant, this implies an inverse scaling between the wing size (c) and frequency (f). Essentially, the wing should not flap slower than the time it takes to shed the leading-edge vortex. This timescale is proportional to the chord, hence the inverse relation between the flapping frequency and the wing size. Later numerical studies confirmed a similar scaling (Lewin & Haj-Hariri 2003). Experiments of oscillating foils including pitching can achieve higher efficiency than the pure symmetric motions discussed here (Anderson et al. 1998).

8. HOVERING

Hovering is an extreme mode of flight where the forward velocity is zero. Insects must figure out how to draw clean air from the ambient flow and manage to get rid of the "messy vortices" to obtain a periodic force. Figure 6 shows the creation of a downward jet by an idealized dragonfly hovering motion (Wang 2000a). The combination of translational and rotational motion solves two problems: to create a dipole, and to get rid of it. A succession of vortex dipoles (or rings in 3D) carries the fluid momentum downward, thereby keeping an insect aloft.

8.1. Two Hovering Styles

In an extensive survey, Weis-Fogh (1973) noticed that most hovering insects, including fruit flies, bees, and beetles, employ symmetric back-and-forth strokes near a horizontal plane. This motion resembles an airfoil or a helicopter wing motion, except that the wing reverses its course periodically. For this reason, Weis-Fogh referred to this style as "normal hovering." A few insects, including some of the best hoverers, true hoverflies and dragonflies, employ asymmetric strokes along

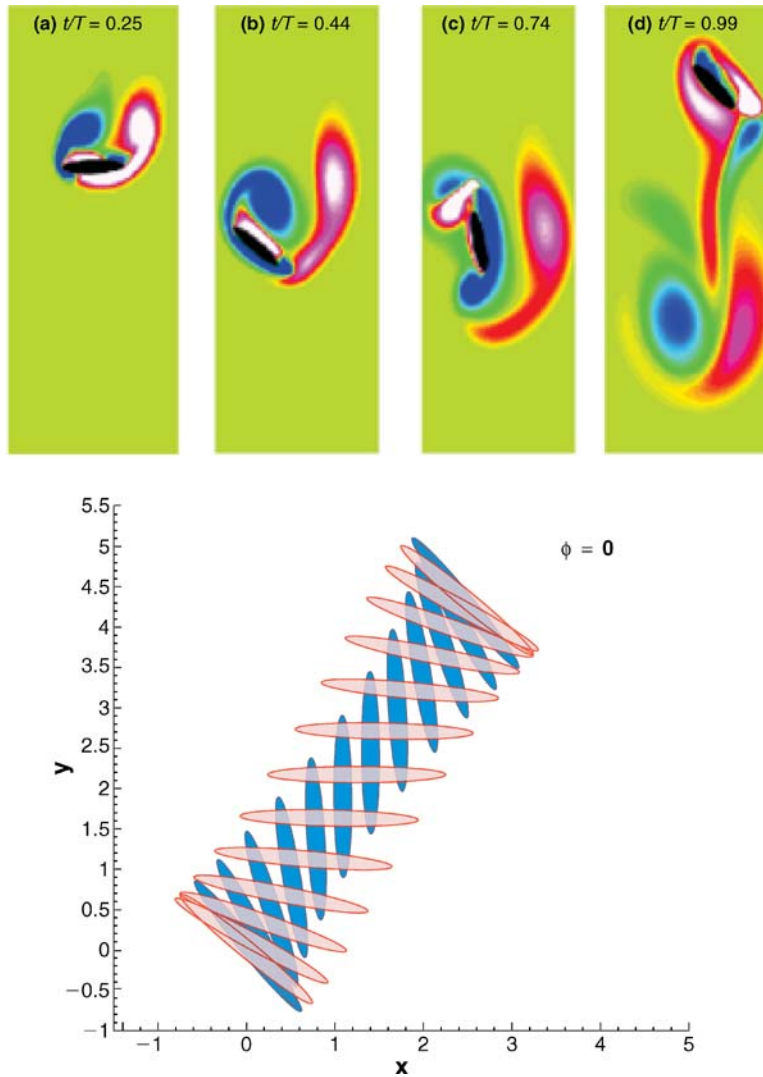

Figure 6 Vorticity field created by a two-dimensional idealized dragonfly wing motion. The schematic on the bottom illustrates the modeled path of the wing section over one full stroke. Orange ovals are the downstroke, blue ones are the upstroke. The four panels on the top show the calculated vorticity generated by the wing (*black*) during the downstroke (*first two panels*) and the upstroke (*next two panels*). Blue represents clockwise vorticity; red represents counterclockwise vorticity. A pair of vortices is tossed down in each wing beat. The lift calculated from the two-dimensional airflows in this model is sufficient to support the weight of a hovering dragonfly (Wang 2000a).

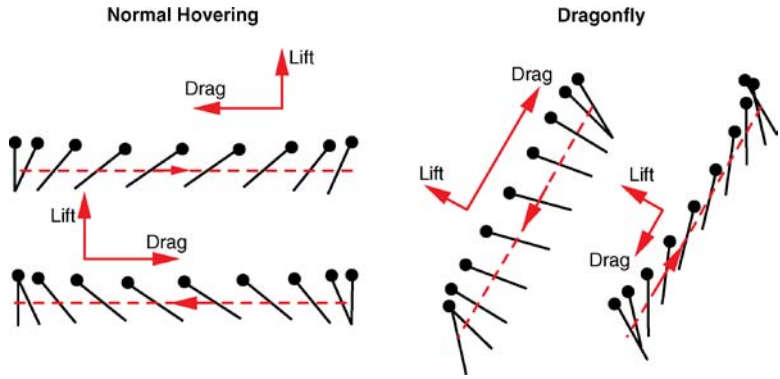

Figure 7 The schematic of two hovering styles. Left: Normal hovering using a horizontal stroke plane. Right: Hovering using an inclined stroke plane.

an inclined stroke plane, resembling a rowing motion, where the force is primarily generated during the down stroke (Figure 7).

This classification has influenced subsequent research in several ways. First, one might argue that because most insects use "normal hovering," it deserves our main attention. Indeed, most experiments and computations have focused on hovering along a horizontal stroke plane (Dickinson et al. 1999, Ellington et al. 1996, Sun & Tang 2002, Wang et al. 2004a). Second, because the upstroke generates little force, one might speculate that the asymmetric strokes are less efficient compared to normal hovering (Weis-Fogh 1973). We re-examine this in section 9.

8.2. Normal Hovering: Dynamic Stall, Rotation, Acceleration, and Wing-Wake Interactions

Using a controlled robotic wing experiment, Dickinson et al. (1999) systematically studied the fluid forces in a family of normal hovering. The motion consists of relatively constant translational velocity in the mid-stroke and rapid accelerations and wing pitch near wing reversal. Thus, during the mid-stroke, the force is dominated by the translational force in dynamic stall regime, whereas near the wing reversal, the force is affected by wing rotation and acceleration. By varying the timing of the rotation with respect to translation, they identified the sources of the force peaks near the wing reversal. One peak depends on the phase between rotation and translation, which is called the rotational force. Its magnitude can be estimated by $C_r U \times \Omega$ (Sane & Dickinson 2002). This has the same form as the lift of a translating and pitching airfoil with small amplitudes (Munk 1925). The second peak is independent of the phase delay and occurs immediately after the wing reversal. This was interpreted as a wake capture. The contribution due to these peaks can be as high as 35% of the total force in some cases. Sun & Tang (2002) computed the forces using similar kinematics to those in Dickinson et al. (1999)

and reported negligible signs of wing-wake interaction after seeing little difference between the force in the first stroke (in the absence of the wake) and in the stroke after the wing reversal. Instead, Sun & Tang (2002) found that these force peaks depend on the acceleration. In contrast, Birch & Dickinson (2003) found noticeable difference in the first and fourth strokes. This discrepancy still requires further investigation.

Theoretically, both the acceleration and wing-wake interaction must have an effect on the forces. However, these effects have eluded simple quantitative prediction, thus making it difficult to estimate their relative strengths. In potential theory, the effect of acceleration can be separated into the classical added mass (Lamb 1945, Sedov 1965) and the force due to shed vorticity (Wagner 1925). With an impulsively accelerated wing, the latter dominates (Pullin & Wang 2004).

It is not clear that the force peaks associated with acceleration are necessarily advantageous to insect flight; the average of the added mass is zero for periodic translational motions, and the simulations of Sun & Tang (2002) show both positive and negative spikes in the lift coefficient, relative to the mean-cycle value, during wing reversal. Another effect worth noting is that an increase in aerodynamic lift due to these unsteady effects is typically accompanied by an increase in drag, see figure 1D in Dickinson et al. (1999) and figure 7 in Wang et al. (2004a). This correlation between the two force components makes sense because the unsteady force in a stalled flow is roughly normal to the wing. This implies that lift enhancement due to these unsteady mechanisms comes at a cost.

8.3. Hovering Along an Inclined Stroke Plane: Dragonfly Flight

Dragonfly hovering was considered an exception to normal hovering because of its use of an up and down asymmetric stroke. Quick estimates based on the blade-element theory predicted an anomalously large lift coefficient, 3.5–6 (Norberg 1975, Weis-Fogh 1973), compared to 1 for normal hovering insects (table 5 in Weis-Fogh 1973). Later inclusion of induced flow in a momentum theory predicted a similarly high value (Ellington 1984). Savage et al. (1979) investigated the effect of the leading-edge vortex using a point vortex model and suggested that its presence was sufficient to explain the required force. Azuma et al. (1985) suggested that the details of dragonfly wing and motion might be what is needed to explain the missing lift. In addition, a few authors have suggested that these unusually high force coefficients might not be unreasonable and could be due to unsteady mechanisms (Somps & Luttges 1985, Freymuth et al. 1991). Somps & Luttges (1985) reported that the peak vertical forces of a tethered dragonfly are about 15–20 times its body weight. Freymuth et al. (1991) estimated the forces on a hovering mechanic wing, based the velocity at far field, and reported a lift coefficient to be 2–7 in normal hovering, although they did not show the force coefficients in dragonfly-like wing motion. On the contrary, 2D computations of dragonfly flight found the vertical force coefficient to be about 2 (normalized by rms value of the velocity), sufficient to support a typical weight of a dragonfly (Wang 2000a). A value of about 2

was also stated in a preliminary 2D computation (Gustavson & Leben 1991) and reported in a recent 3D computation of dragonfly flight (Sun & Lan 2004).

Recently, Wang (2004) suggested that the anomalously large coefficients are a consequence of underestimating drag. In the previous quasi-steady analyses, drag was assumed to be much smaller than lift. For example, the lift-to-drag ratio was assumed to be about 7 in Weis-Fogh (1973), and 6 in Norberg (1975). These were estimates based on the maximal value of lift-to-drag ratio from experiments on a locust wing (Jensen 1956). Ellington (1984) used the relation $C_{D,pro} \sim 7/\sqrt{\mathrm{Re}}$ based on flow past a cylinder and deduced a value of 0.15–0.2 at Re around 10^3 for the profile drag coefficient. While these values might be reasonable at small angles of attack, they are underestimates of drag at stalled angles during the downstroke. In the case of hovering along an inclined stroke plane, the drag during down stroke can support about 76% of the weight (Wang 2004). Therefore, assuming a lift-to-drag ratio of 6.5 effectively ignores about 72% (76%–24%/6.5) of the net vertical force. This would require a factor of 4 increase in the lift coefficient to compensate. Including the appropriate amount of drag, Norberg's (1975) estimate, $C_L \sim 3.5$–6.1, would lead to a lift coefficient of about 0.9–1.5, which is comparable to that of a normal hovering insect. Incidentally, the underestimate of drag would not affect the lift estimates in normal hovering, where the drag cancels in two consecutive half strokes.

9. LIFT, DRAG, AND EFFICIENCY

The separation of lift and drag was convenient for an airfoil for at least two reasons. First, at a small angle of attack, the lift is many times the drag. Second, in steady forward flight, the efficiency is measured by the lift-to-drag ratio. Neither of these applies to a hovering insect. At a large angle of attack, the lift and drag are of comparable magnitude. In addition, except in the case of a strictly horizontal stroke plane, the lift-to-drag ratio is no longer a measure of the efficiency (Wang 2004).

This discussion of lift and drag may, at first, seem a matter of semantics. Presumably an insect does not differentiate lift and drag. However, a reconsideration of the role of drag helps us to propose a strategy to improve hovering efficiency (Wang 2004). Instead of using both half strokes, take a half stroke and make it a down stroke by tilting the stroke plane such that the net force points vertically up (Figure 8). The upstroke simply returns to the starting position with a zero angle of attack. Consider a special limit, where we assume that the return stroke is free and the lift-to-drag ratio is 1; it follows that a half stroke consumes less power, by a factor of $\sqrt{2}/2$, than the full stroke to support a given weight.

This example has two implications. First, as mentioned in the introduction, the view of insect flight as "rowing" was dismissed because it was considered inefficient. However, if an insect wing has a constraint on the stroke amplitude and frequency, it might have to employ a large angle of attack to generate sufficient

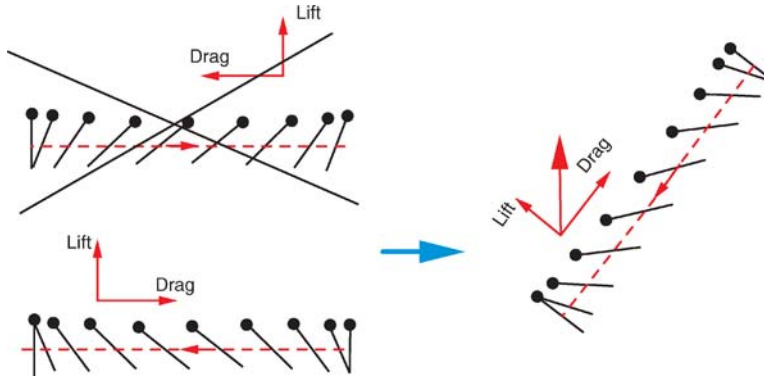

Figure 8 Saving power by eliminating a half stroke in normal hovering (Wang 2004).

forces. In this limit, the rowing-like stroke can be more efficient than the back-and-forth airfoil action. Second, a normal hovering along a strict horizontal stroke plane has an artifact that the drag is canceled in two half strokes. The wing-tip motion observed in insects, whether a figure eight, an ellipse, or a parabola, all have a plunging down portion during which the drag has an upward component. The deviation of the stroke plane from a horizontal plane is similar in spirit to rotating a half stroke in the above example.

10. PASSIVE FLAPPING FLIGHT

In the cases discussed so far, the wing follows our instructions. What happens if we let the wing go about its way in a fluid? Figure 9 shows a piece of free-falling paper in air, where a periodic motion rises without being prescribed nor driven by a periodic force (Pesavento & Wang 2004). In this sense, a piece of falling paper is a special case of flapping flight where the driving force is constant.

Free falling plates in a fluid can also be used to test models of fluid forces (Pesavento & Wang 2004; A. Andersen, U. Pesavento & Z.J. Wang, submitted). Tracking the fall of plates provides both its motion and the fluid force (determined from the acceleration). Interestingly, the force on the tumbling plate shown in Figure 9 is dominated by the term that scales $U \times \Omega$ rather than U^2, which is expected for classical Phugoids (Lanchester 1910). This is also in contrast with the force in prescibed motions, which are typically dominated by the term proportional to U^2 (Wang et al. 2004a).

An example where an insect wing can benefit from passive interactions with fluids is during wing rotation. Russell & Wang (in preparation) found that the pronation of a dragonfly wing is primarily due to fluid torque and thus is passive. This would explain a torsional wave from tip to root as seen in the experiments and previous observations described in section 3.1.

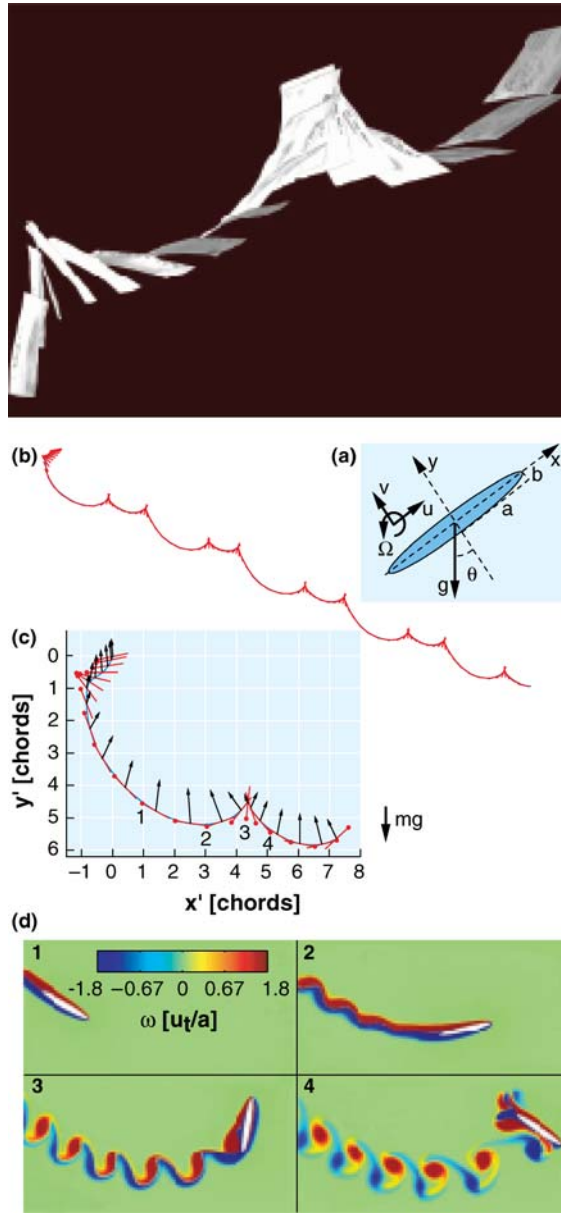

Figure 9 Falling Paper: Navier-Stokes Solutions, Model of Fluid Forces, and Center of Mass Elevation. Top: Falling paper filmed at 300 fps under windless conditions. Bottom: The Navier-Stokes solution of a tumbling ellipse. (*a*) Coordinate system, (*b*) trajectory of the chord (in *red*) in the first five periods released from rest, (*c*) instantaneous fluid forces (*black*) superposed on the chords (*red*), and (*d*) vorticity field at four instants during a full rotation (Pesavento & Wang 2004).

11. CONCLUDING REMARKS

"What force does an insect wing generate" has been the driving force behind much of the research described here. An innocent question, but a difficult one to answer. The difficulty is, in part, due to our lack of simple theories of unsteady fluids stirred by a moving geometry. In search for the answer, we are forced to explore solutions beyond the classical theories and develop appropriate tools. One hopes that the insight gained in studying insect flight might lead to our finding efficient ways to interact with fluids. Besides insects, birds, fish, leaves, flags, kites, sails, oars, and heart valves, all live in fluids and encounter a similar set of problems.

Understanding force generation on a flapping wing, though a difficult feat, is only a beginning of our understanding of insects or flapping flight in nature as a whole. "Why do insects or birds flap their wings the way they do? " and "how does flapping flight come about in the course of evolution? " For us who are bound to Earth, to fly like birds may always be a temptation. Fundamental to such an endeavor are efficiency and stability (Lanchester 1910, Lilienthal 1911). "Can flapping flight be more efficient and stable than a fixed-wing flight?"

ACKNOWLEDGMENTS

I am grateful to Steve Childress for initiating my interest in this fascinating problem and subsequent collaboration. I thank Michael Dickinson, Charles Peskin, and Dale Pullin for sharing their valuable expertise in our collaborations, and Andy Ruina for helpful discussions. The work is supported by AFOSR, an NSF Early Career Award, an ONR Young Investigator Award, and a David and Lucille Packard Fellowship.

The *Annual Review of Fluid Mechanics* is online at http://fluid.annualreviews.org

LITERATURE CITED

Alexander DE. 1984. Unusual phase relationships between the forewings and hindwings in flying dragonflies. *J. Exp. Biol.* 109:379–83

Anderson JM, Streitlien K, Barrett DS, Triantafyllou MS. 1998. Oscillating foils of high propulsive efficiency. *J. Fluid Mech.* 360:41

Azuma A, Azuma S, Watanabe I, Furuta T. 1985. Flight mechanics of a dragonfly. *J. Exp. Biol.* 116:79–107

Birch J, Dickinson MH. 2001. Spanwise flow and the attachement of the leading-edge vortex on insect wings. *Nature* 412:729–33

Birch JM, Dickinson MH. 2003. The influence of wing-wake interactions on the production of aerodynamic forces in flapping flight. *J. Exp. Biol.* 206:2257–72

Brodsky AK. 1994. *The Evolution of Insect Flight.* Oxford: Oxford Univ. Press

Childress S. 1981. *Swimming and Flying in Nature.* Cambridge: Cambridge Univ. Press

Childress S, Dudley R. 2004. Transition from ciliary to flapping mode in a swimming mollusc: flapping flight as a bifurcation in Re_ω. *J. Fluid Mech.* 498:257–88

Cloupeau M, Devillers JF, Devezeaux D. 1979.

Direct measurements of instantaneous lift in desert locust: comparison with Jensen's experiments on detached wings. *J. Exp. Biol.* 80:1–15

Dalton S. 1975. *Borne on the Wind*. New York: Reader's Digest Press

Demoll R. 1918. Der flug der insekten und der vögel. *Jena: G. Fisher*

Dickinson MH. 1996. Unsteady mechanisms of force generation in aquatic and aerial locomotion. *Am. Zool.* 36:537–54

Dickinson MH, Götz KG. 1993. Unsteady aerodynamic performance of model wings at low reynolds numbers. *J. Exp. Biol.* 174:45–64

Dickinson MH, Götz KG. 1996. The wake dynamics and flight forces of the fruit fly *Drosophilia Melanogaster*. *J. Exp. Biol.* 199:2085–104

Dickinson MH, Lehmann FO, Sane SP. 1999. Wing rotation and the aerodynamic basis of insect flight. *Science* 284:1954–60

Dudley R. 1998. *The Biomechanics of Insect Flight: Form, Function, Evolution*. Princeton: Princeton Univ.

Dudley R, Ellington CP. 1990. Mechanics of forward flight in bumblebees ii. quasi-steady lift and power requirements. *J. Exp. Biol.* 148:53

Ellington CP. 1984. The aerodynamics of hovering insect flight i.-v. *Phil. Trans. R. Soc. London* B305:1–181

Ellington CP. 1995. Unsteady aerodynamics of insect flight. In *Biological Fluid Dynamics*, ed. CP Ellington, TJ Pedley, Vol. 109, p. 129. Soc. Exp. Biol.

Ellington CP, van den Berg C, Willmott AP, Thomas ALR. 1996. Leading-edge vortices in insect flight. *Nature* 384:626–30

Francis RH, Cohen J. 1933. The flow near a wing which starts suddenly from rest and then stalls. *Aero. Res. Council Rep. Mem.* No. 1561, 90

Freymuth P, Gustafson K, Leben R. 1991. Visualization and computation of hovering mode. In *Votex Method and Vortex Motion*, ed. K Gustavson, J Sethian, p. 143. Philadelphia: SIAM

Fry SN, Sayaman R, Dickinson MH. 2003. The aerodynamics of free-flight manuevers in *Drosophila*. *Science* 300:495–98

Glauert H. 1929. The force and moment on an oscillationg aerofoil. *Tech. Rep. Aero. Res. Comm.* No. 1242, 742

Glauert H. 1947. *The Elements of Aerofoil and Airscrew Theory*. Cambridge: Cambridge Univ. Press

Greenewalt CH. 1962. *Dimensional Relationships for Flying Animals*, Vol. 144. Washington, DC: Smithsonian Misc. Collections

Gustavson K, Leben R. 1991. Computation of dragonfly aerodynamics. *Comput. Phys. Commun.* 65:121

Harris F. 1966. Preliminary study of radial flow effects on rotor blades. *Am. Helicopter Soc.* 11:1–21

Hollick FSJ. 1940. The flight of the dipterous fly muscina stabulans fallen. *Phil. Trans. R. Soc. B* 230:357–90

von Holst E, Kuchemann D. 1941. Biological and aerodynamical problems of animal flight. *Die Naturwissenschaft* 29:348–62

Iima M, Yanagita T. 2001. An analysis of a symmetric flapping model: a symmetry-breaking mechanism and its universality. *Theor. Appl. Mech.* 50:237–45

Jensen M. 1956. Biology and physics of locust flight. iii. The aerodynamics of locust flight. *Proc. R. Soc. B. 239* 239:511–52

Jones M. 2003. The separated flow of an inviscid fluid around a moving flat plate and the unsteady kutta condition. *J. Fluid Mech.* 496:405–41

von Karman T, Burgers JM. 1963. General aerodynamic theory—perfect fluids. In *Aerodynamic Theory*, ed. W Durand, Vol. 2, Div. E. Berlin: Springer

von Karman T, Sears WR. 1938. Airfoil theory for non-uniform motion. *J. Aeronaut. Sci.* 5(10):379–90

Lamb H. 1945. *Hydrodynamics.* New York: Dover

Lanchester FW. 1910. *Aerodonetics.* New York: D. Van Nostrand

Lehman FO. 2004. The mechanisms of lift enhancement in insect flight. *Naturwissenschaften* 91:101–22

Lewin GC, Haj-Hariri H. 2003. Modelling thrust generation of a two-dimensional heaving airfoil in a viscous flow. *J. Fluid Mech.* 492:339–62

Liao J, Beal D, Lauder G, Triantafyllou M. 2003. The karman gait: novel body kinematics of rainbow trout swimming in a vortex street. *Science* 206:1059–73

Lighthill MJ. 1973. On the weis-fogh mechanism of lift generation. *J. Fluid Mech.* 60:1

Lighthill MJ. 1975. *Mathematical Biofluiddynamics*. Philadelphia: Soc. Ind. Appl. Math.

Lilienthal O. 1911. *Birdflight as the Basis of Aviation*. London: Longmans & Green

Liu H, Ellington C, Kawachi K, van den Berg C, Willmott AP. 1998. A computational fluid dynamic study of hawkmoth hovering. *J. Exp. Biol.* 201:461

Magnan A, Sainte-Laguë A. 1933. La vol au point fixe. *Actualites Sci. Ind.* 60

Marey EJ. 1868a. Determination experimentale du mouvement des ailes des insectes pendant le vol. *C. R. Acad. Sci. Paris* 67:1341–45

Maxworthy T. 1979. Experiments on the Weis-Fogh mechanism of lift generation by insects in hovering flight. *J. Fluid Mech.* 93:47–63

Maxworthy T. 1981. The fluid dynamics of insect flight. *Annu. Rev. Fluid Mech.* 13:329

Miller L, Peskin C. 2004. When vortices stick: an aerodynamic transition in tiny insect flight. *J. Exp. Biol.* 207:3073–88

Minotti FO. 2002. Unsteady two-dimensional theory of a flapping wing. *Phys. Rev. E* 66: 051907–17

Mohseni K, Gharib M. 1998. A model for universal time scale of vortex ring formation. *Phys. Fluids* 10:2436–38

Munk MM. 1925. Note on the air forces on a wing causd by pitching. In *Technical notes: National advisory committee for aeronautics paper.* 217:1–6

Nachtigall W. 1966. Die kinematik der schlagfügelbewegungen von dipteren. Methoddische und analyticshe grundlagen zur biophysik des insektenflugs. *Z. Vergl. Physilo.* 52:155–211

Nachtigall W. 1974. *Insects in Flight.* New York: McGraw-Hill

Nachtigall W. 1977. Die aerodynamisch polare des tipula-flugels und eine einrichtung zur halbautomatischen polarenaufnahme. In *The Physiology of Movement: Biomechanics*, ed. W Nachtigall, pp. 347–52 Stuttgart: Fischer

Norberg RA. 1972. The pterostigma of insect wings as inertial regulator of wing pitch. *J. Comp. Physiol.* 81(1):9–22

Norberg RA. 1975. Hovering flight of the dragonfly aeschna juncea l., kinematics and aerodynamics. In *Swimming and Flying in Nature*, ed. TY Wu, CJ Brokaw, C Brennen. 2:763–80

Osborne MFM. 1951. Aerodynamics of flapping flight with application to insects. *J. Exp. Biol.* 47:561

Pesavento U, Wang ZJ. 2004. Falling paper: Navier-Stokes solutions, model of fluid forces, and center of mass elevation. *Phys. Rev. Lett.* In press

Prandtl L, Tietjens OG. 1957. *Applied Hydro- and Aeromechanics*. New York: McGraw-Hill

Pringle J. 1957. *Insect Flight*. Cambridge: Cambridge Univ. Press

Pullin DI. 1978. The large-scale structure of unsteady self-similar rolled-up vortex sheets. *J. Fluid Mech.* 88:401

Ramamurti R, Sandberg WC. 2002. A three-dimensional computational study of the aerodynamic mechanisms of insect flight. *J. Exp. Biol.* 205:1507–18

Rayner J. 1979a. A vortex theory of animal flight. Part 1. The vortex wake of a hovering animal. *J. Fluid Mech.* 91:697

Rayner J. 1979b. A vortex theory of animal flight. Part 2. The forward flight of birds. *J. Fluid Mech.* 91:731

Ruppell G. 1989. Kinematic analysis of symmetrical flight maneuvres of odonata. *J. Exp. Biol.* 144:13–42

Russell D, Wang ZJ. 2003. A cartesian grid method for modeling multiple moving irregular objects in two dimensional incompressible viscous flow. *J. Comp. Phys.* 191:177–205

Sane S. 2003. The aerodynamics of insect flight. *J. Exp. Biol.* 206:4191–208

Sane S, Dickinson MH. 2002. The aerodynamic effects of wing rotation and a revised quasi-steady model of flapping flight. *J. Exp. Biol.* 205:1087–96

Savage S, Newman BG, Wong DTM. 1979. The role of vortices and unsteady effects during the hovering flight of dragonflies. *J. Exp. Biol.* 83:59–77

Schlichting H. 1979. *Boundary-Layer Theory*. New York: McGraw-Hill

Sedov LI. 1965. *Two Dimensional Problems in Hydrodynamics and Aerodynamics*. New York: Interscience

Somps C, Luttges MW. 1985. Dragonfly flight: novel uses of unsteady separated flows. *Science* 228:1326–28

Spedding GR. 1992. The aerodynamics of flight. In *Mechanics of Animal Locomotion*, pp. 52–107. Berlin: Springer-Verlag

Spedding GR, Rosen M, Hedenström A. 2003. A family of vortex wakes generated by a thrust nightingale in free flight in a wind tunnel over its entire natural range of flight speeds. *J. Exp. Biol.* 206:2313–44

Srygley RB, Thomas AL. 2002. Unconventional lift-generating mechanisms in free-flying butterflies. *Nature* 420:660–64

Sun M, Lan S. 2004. A computational study of the aerodynamic forces and power requirements of dragonfly (*aeschna juncea*) hovering. *J. Exp. Biol.* 207:1887–901

Sun M, Tang J. 2002. Unsteady aerodynamic force generation by a model fruit fly wing in flapping motion. *J. Exp. Biol.* 205:55–70

Usherwood JR, Ellington CP. 2002a. The aerodynamics of revolving wings i. model hawkmoth wings. *J. Exp. Biol.* 205:1547–64

Usherwood JR, Ellington CP. 2002b. The aerodynamics of revolving wings ii. propeller force coefficients from mayfly to quail. *J. Exp Biol.* 205:1565–76

Vandenberghe N, Zhang J, Childress S. 2004. Symmetry breaking leads to forward flapping flight. *J. Fluid. Mech.* 506:147–55

Vogel S. 1967a. Flight in drosophila ii. variations in stroke parameters and wing contour. *J. Exp. Biol.* 46:383–92

Vogel S. 1967b. Flight in drosophila iii. aerodynamic characteristics of fly wings. *J. Exp. Biol.* 46:431–43

Vogel S. 1996. *Life in Moving Fluids*. Princeton, NJ: Princeton Univ.

Wagner H. 1925. Über die entstehung des dynamischen auftriebes von tragflüeln. *Z. angew. Math. Mech.* 5:17–35

Wakeling JM, Ellington CP. 1997. Dragonfly flight ii: velocities, accelerations and kinematics of flapping flight. *J. Exp. Biol.* 200:557–82

Walker GT. 1925. The flapping of birds. *J. R. Aero. Soc.* 29:590–94

Walker PB. 1931. Experiments on the growth of circulation about a wing. *ARC Tech. Rep.* No. 1402

Wang H, Zeng L, Liu H, Yin C. 2003. Measuring wing kinematics, flight trajectory and body attitude during forward flight and turning maneuvers in dragonflies. *J. Exp. Biol.* 206:745–57

Wang ZJ. 2000a. Two dimensional mechanism of hovering. *Phys. Rev. Lett.* 85:2216–19

Wang ZJ. 2000b. Vortex shedding and frequency selection in flapping flight. *J. Fluid Mech.* 410:323–41

Wang ZJ. 2004. The role of drag in insect hovering. *J. Exp. Biol.* In press

Wang ZJ, Birch J, Dickinson MH. 2004a. Unsteady forces in hovering flight: computation vs experiments. *J. Exp. Biol.* 207:449

Wang ZJ, Childress S, Cowen N, Peskin C. 2003b. *The take-off of a pair of flexible wings driven by muscles.* Presented at Am. Phys. Soc. Div. Fluid Dyn. Meet., Meadowlands, NJ

Weis-Fogh T. 1973. Quick estimates of flight fitness in hovering animals, including novel mechanisms for lift production. *J. Exp Biol.* 59:169–230

Weis-Fogh T, Jensen M. 1956. Biology and physics of locust flight. i. basic principles in insect flight. a critical review. *Proc. R. Soc. B.* 239:415–58

Wilkin PJ. 1990. The instantaneous force on a desert locust, schistocerca gregaria (orthoptera: Acrididae), flying in a wind tunnel. *J. Kansas Entomol. Soc.* 63316–28

Wilkin PJ, Williams MH. 1993. Comparison of the instantaneous aerodynamic forces on a sphingid moth with those predicted by quasi-steady aerodynamic theory. *Physiol. Zool.* 66:1015–44

Willmott AP, Ellington CP. 1997a. The mechanics of flight in the hawkmoth manduca sexta i. kinematics of hovering and forward flight. *J. Exp Biol.* 200:2705–22

Willmott AP, Ellington CP. 1997b. The mechanics of flight in the hawkmoth manduca sexta ii. aerodynamic consequences of kinematic and morphological variation. *J. Exp Biol.* 200:2723–45

Wootton RJ. 1981. Support and deformability in insect wings. *J. Zool.* 193:447–68

Wu JC. 1981. Theory for Aerodynamic Force and Moment in Viscous Flows. *AIAA* 19: 432–41

Wu T. 2001. On theoretical modeling of aquatic and aerial animal locomotion. *Adv. Appl. Mech.* 38:291–353

Zanack W. 1972. Flugbiophysik der wanderheuschrecke (*locusta migratoria l.*). *J. Comp. Physiol.* 78(4):356–95

Zanker JM, Götz KG. 1990. The wing beat of drosophilia melanogaster ii. dynamics. *Phil. Trans. R. Soc London B.* 327:19–44

Zhang J, Childress S, Libchaber A, Shelley M. 2000. Flexible filaments in a flowing soap film as a model for one-dimensional flags in a two-dimensional wind. *Nature* 408:835–39

Annual Review of Fluid Mechanics
Volume 37, 2005

CONTENTS